Published OnlineFirst July 30, 2020; DOI: 10.1158/1078-0432.CCR-20-0389

Stimulation of Oncogene-Specific Tumor-Infiltrating T Cells through Combined Vaccine and αPD-1 Enable Sustained Antitumor Responses against Established HER2 Breast Cancer

Erika J. Crosby[1], Chaitanya R. Acharya[1], Anthony-Fayez Haddad[1], Christopher A. Rabiola[1], Gangjun Lei[1], Jun-Ping Wei[1], Xiao-Yi Yang[1], Tao Wang[1], Cong-Xiao Liu[1], Kay U. Wagner[2], William J. Muller[3], Lewis A. Chodosh[4], Gloria Broadwater[5], Terry Hyslop[5], Jonathan H. Shepherd[6,7], Daniel P. Hollern[6,7], Xiaping He[6,7], Charles M. Perou[6,7], Shengjie Chai[6,8], Benjamin K. Ashby[6,8], Benjamin G. Vincent[6,8,9,10], Joshua C. Snyder[1,11], Jeremy Force[12], Michael A. Morse[12], Herbert K. Lyerly[1,13,14], and Zachary C. Hartman[1,14]

ABSTRACT

Purpose: Despite promising advances in breast cancer immunotherapy, augmenting T-cell infiltration has remained a significant challenge. Although neither individual vaccines nor immune checkpoint blockade (ICB) have had broad success as monotherapies, we hypothesized that targeted vaccination against an oncogenic driver in combination with ICB could direct and enable antitumor immunity in advanced cancers.

Experimental Design: Our models of HER2$^+$ breast cancer exhibit molecular signatures that are reflective of advanced human HER2$^+$ breast cancer, with a small numbers of neoepitopes and elevated immunosuppressive markers. Using these, we vaccinated against the oncogenic HER2Δ16 isoform, a nondriver tumor-associated gene (GFP), and specific neoepitopes. We further tested the effect of vaccination or anti–PD-1, alone and in combination.

Results: We found that only vaccination targeting HER2Δ16, a driver of oncogenicity and HER2-therapeutic resistance, could elicit significant antitumor responses, while vaccines targeting a nondriver tumor-specific antigen or tumor neoepitopes did not. Vaccine-induced HER2-specific CD8$^+$ T cells were essential for responses, which were more effective early in tumor development. Long-term tumor control of advanced cancers occurred only when HER2Δ16 vaccination was combined with αPD-1. Single-cell RNA sequencing of tumor-infiltrating T cells revealed that while vaccination expanded CD8 T cells, only the combination of vaccine with αPD-1 induced functional gene expression signatures in those CD8 T cells. Furthermore, we show that expanded clones are HER2-reactive, conclusively demonstrating the efficacy of this vaccination strategy in targeting HER2.

Conclusions: Combining oncogenic driver targeted vaccines with selective ICB offers a rational paradigm for precision immunotherapy, which we are clinically evaluating in a phase II trial (NCT03632941).

Introduction

Immune checkpoint blockade (ICB) via mAbs targeting the PD-1/PD-L1 interaction has demonstrated a clinical benefit in patients with metastatic disease across many malignancies (1). However, these therapeutic responses are limited to a subset of patients, with ICB responsiveness being associated with the presence of effector tumor-infiltrating lymphocytes (TILs) or a high number of somatic mutations encoding for clonal neoepitopes (2–4). This dichotomy is exemplified in breast cancer, which is composed of multiple molecular subtypes within a single tissue environment that each exhibit differential responses to ICB (5). PD-L1 ICB has demonstrated antitumor activity in some triple-negative breast cancers (TNBCs), a subtype with elevated levels of p53 mutations, high TILs, and increased neoepitope burden (6, 7). This is in contrast to the hormone receptor (HR$^+$) and HER2$^+$ molecular subtypes of breast cancer, which have distinct oncogenic drivers, generally contain fewer neoepitopes and TILs, and have shown lower response rates to ICB than TNBC (5, 8). As HR$^+$ and HER2$^+$ subtypes are highly dependent upon the expression of their respective oncogenes, these subtypes present an opportunity to therapeutically target essential, nonmutated driver genes (9). Rather than relying on the presence of endogenous T-cell responses, this type of vaccine strategy could be used to actively induce and direct oncogene-specific adaptive immunity.

Although HER2 is expressed in many cell types, it is highly amplified in HER2$^+$ breast cancer and is not just a marker of tumorigenesis but is

[1]Department of Surgery, Division of Surgical Sciences, Duke University, Durham North Carolina. [2]Department of Oncology, Wayne State University, Barbara Ann Karmanos Cancer Institute, Detroit, Michigan. [3]Departments of Biochemistry and Medicine, Goodman Cancer Center, McGill University, Montreal, Quebec. [4]Department of Cancer Biology, University of Pennsylvania, Philadelphia, Pennsylvania. [5]Department of Biostatistics and Bioinformatics, Duke University, Durham, North Carolina. [6]Lineberger Comprehensive Cancer Center, University of North Carolina, Chapel Hill, North Carolina. [7]Department of Genetics, University of North Carolina, Chapel Hill, North Carolina. [8]Department of Medicine, Division of Hematology/Oncology, University of North Carolina, Chapel Hill, North Carolina. [9]Curriculum in Bioinformatics and Computational Biology, University of North Carolina, Chapel Hill, North Carolina. [10]Computational Medicine Program, University of North Carolina, Chapel Hill, North Carolina. [11]Department of Cell Biology, Duke University, Durham, North Carolina. [12]Department of Medicine, Duke University, Durham, North Carolina. [13]Department of Immunology, Duke University, Durham, North Carolina. [14]Department of Pathology, Duke University, Durham, North Carolina.

Note: Supplementary data for this article are available at Clinical Cancer Research Online (http://clincancerres.aacrjournals.org/).

Corresponding Author: Zachary C. Hartman, Duke Medical Center, MSRB I Box 2606, Durham, NC 27710. Phone: 919-613-9110; Fax: 919-681-7970; E-mail: Zachary.hartman@duke.edu

Clin Cancer Res 2020;XX:XX–XX

doi: 10.1158/1078-0432.CCR-20-0389

Published OnlineFirst July 30, 2020; DOI: 10.1158/1078-0432.CCR-20-0389

Translational Relevance

This study demonstrates two fundamental tenets of immunotherapy: vaccines targeting any tumor antigen will not be as effective as those targeting true oncogenic drivers and neither the stimulation of tumor-specific T cells nor the blockade of a key immune checkpoint is enough to overcome the layers of immune suppression by itself. We provide single-cell genetic evidence that vaccination alone generates a population of CD8 T cells incapable of long-term tumor control due to the activation of numerous immune dysfunction pathways within the tumor. These promising studies have led to the initiation of a phase II clinical trial testing a novel HER2 vaccine in combination with pembrolizumab (NCT03632941) to determine whether this combination can elicit effective antitumor immunity while minimizing off-target immune responses in patients with advanced HER2$^+$ breast cancer.

recognized as an oncogenic driver (10). However, multiple reports have identified a particularly oncogenic isoform of HER2 that lacks exon 16 (HER2Δ16), which can constitutively dimerize to confer sustained cellular signaling (11–14). Although the importance of HER2Δ16 in patient samples is not clear, amplification of HER2 may result in elevated expression of this isoform sufficient to transform cells (13). Clinical use of HER2 mAbs has demonstrated the importance of engaging HER2-specific innate immune responses for antitumor efficacy (9, 15), while multiple clinical vaccine trials (using both viral vectors and peptides) have suggested the importance of eliciting HER2-directed T-cell responses in antitumor immunity (16–18). We hypothesized that immunologically targeting the oncogenic HER2Δ16 isoform may be a particularly attractive option due to its importance in maintaining tumor signaling. In our past studies, we found that a HER2-specific viral vaccine can enhance progression-free survival in patients with recurrent HER2$^+$ metastatic breast cancer (18). Here, we altered our vaccine to target the HER2Δ16 isoform to determine whether this strategy could better elicit adaptive responses in comparison to targeting nondriver, tumor-specific genes or unique tumor neoepitopes. We further wanted to determine whether this vaccine would synergize with PD-1 ICB to allow for enhanced antitumor immunity in a model of advanced HER2$^+$ breast cancer.

In these studies, we establish evidence of HER2Δ16 isoform expression in clinical samples of breast cancer and confirm that this isoform functions as a potent oncogenic driver to transform breast epithelial cells. Using a HER2Δ16 transgenic mouse model, we determined that the spontaneous tumors that formed were largely nonmutated HER2$^+$ breast cancer with immunosuppressive molecular signatures, reflective of advanced human HER2$^+$ breast cancer (14). We demonstrate that vaccination targeting the extracellular domain of HER2Δ16 was essential to elicit effective antitumor immunity, but that this effect was diminished in established tumors. Likewise, we found that established endogenous tumors failed to respond to αPD-1 monotherapy, mirroring early clinical findings (5). However, the combination of HER2Δ16 vaccination with αPD-1 treatment led to long-term tumor-free survival and the activation of HER2-specific T cells in the tumor microenvironment (TME) of established tumors without the induction of an exhaustion signature that was present when the vaccine was given alone. This supports an approach targeting oncogenes with vaccines combined with systemic ICB to offer an effective, scalable means to achieve precision immunotherapy in advanced cancers. These results supported the combination of αPD-1 with our previously published viral HER2 vaccine to validate these findings in patients with advanced breast cancer (NCT03632941, currently enrolling).

Materials and Methods

Cell lines and signaling assays

Tumor cell lines MM3MG, NMUMG, EPH4, 293T, and Jurkat were obtained from and maintained as recommended by the ATCC. Cells were modified by stable lentivirus transduction and selection for expression of indicated genes. CRISPR-Cas9 lentiviruses were used to knockout mouse PD-L1, checked by sequencing and flow cytometry. In signaling assays, 293T cells stably expressing dox-inducible HER2 isoforms were transfected with dual luciferase reporter constructs (Cignal Reporter Assay Kit, 336841, Qiagen) and harvested at 24 to 48 hours for luciferase activity. Each condition was plated in quadruplicate and GFP control vectors were used as negative controls.

Mouse experiments

Human HER2-transgenic mice (C57BL/6 background; kindly provided by Dr. Wei-Zen Wei, Wayne State University, Detroit, MI; ref. 19) were crossed with BALB/c mice (000651, The Jackson Laboratory) and MM3MG cells were implanted into the mammary fat pads (1×10^5 cells) of 6- to 10-week-old F1 generation mice. Tumor measurements were made using calipers and volumes calculated using the formula [v = width × width × (length/2)]. Vaccinations were given by footpad injection of 2.6×10^{10} adenoviral particles/mouse. Peptides for peptide vaccines were mixed 1:1 with montanide and given weekly, twice subcutaneously (100 μg/peptide) and once in the footpad (20 μg/peptide). The HER2Δ16 transgenic mouse model was generated by crossing two different strains of mice, TetO-HER2Δ16-IRES-EGFP (a kind gift from W.J. Muller; ref. 14) and MMTV-rtTA (a kind gift from Dr. Lewis A. Chodosh; ref. 14) or MMTV-tTA (a kind gift from K.-U. Wagner; ref. 21) to generate TET-ON or TET-OFF expression of HER2Δ16 to drive spontaneous tumor formation. In TET-ON mice, mice older than 6 weeks were put on a doxycycline-containing diet (200 mg/kg, Bio-Serv). Individual animals were either vaccinated 1 week postinduction (early prevention model) or randomly enrolled into a specific treatment group as soon as palpable breast tumors were detected (~200 mm^3) in any of the eight mammary fat pads. Animals were terminated once any single tumor volume reached >2,000 mm^3. Mice treated with αPD-1 were given 200 μg i.p. weekly. All mouse experiments were done in accordance with Duke Institutional Animal Care and Use Committee–approved protocols.

RNA sequencing alignment, quantification, and neoantigen prediction

Library preparation and sequencing was performed by Admera. Libraries were created using SureSelect XT Mouse All Exon Kit (Agilent) according to the manufacturer's instructions. RNA expression from HER2Δ16 tumors was compared with RNA sequencing (RNA-seq) data from 175 other murine mammary and tumor samples listed in Supplementary Table S1A. All murine RNA-seq data have been deposited in the NCBI GEO accession number GSE148482. Matched normal DNA extracted from tail clippings was respectively derived. Bioinformatics prediction of neoantigens was performed as described previously (22, 23). Predicted neoantigens were filtered on expression in all replicates with >5 × read support.

Library preparation for single-cell RNA-seq

Tumors from treated transgenic mice were harvested and processed into single-cell suspension using Mouse Tumor Dissociation Kit

Published OnlineFirst July 30, 2020; DOI: 10.1158/1078-0432.CCR-20-0389

(Miltenyi Biotec) following the manufacturer's protocol with recommendations for 10X Genomics platform use. Red blood cells were lysed with ACK lysing buffer (Thermo Fisher Scientific) for 5 minutes, and stained with Fixable Far Red Dead Cell Stain (Thermo Fisher Scientific) and antibodies for CD45 (30F11), CD8β (YTS156.7.7), CD4 (RM4-5; all BioLegend). Live, single, $CD45^+$, CD4, and/or $CD8^+$ cells from tumor suspension were sorted by FACS. 10X libraries were created using Chromium Single Cell 5′ Library Construction Kit (v1.0) following the manufacturer's protocol. A targeted cell recovery of 3,000 cells was used for each tumor sample. Both gene expression and V(D)J enrichment libraries were created for each sample. Generated cDNA and final GEX/TCR libraries were quality checked using an Agilent Bioanalyzer 2100 and submitted to MedGenome Inc for sequencing on a NovaSeq S4 instrument.

Single-cell RNA-seq analysis

Fastq files from 10X library sequencing were processed using the CellRanger pipeline (10x Genomics, version 2.1.0) by MedGenome Inc. Filtered gene-barcode matrices that contained only barcodes with unique molecular identifier (UMI) counts that passed the threshold for cell detection were used for further analysis. We followed Seurat's (version 3.1.2; ref. 24) data integration procedure (see Supplementary Methods for complete details), which is designed to integrate diverse single-cell datasets. Seurat returned a corrected data matrix for all datasets, which was used for subsequent analyses.

Expanded clone TCR reactivity test

Aligned sequences from expanded clones were extracted using CellRanger (10× Genomics; Supplementary Table S1E) cloned into vectors containing GFP. These constructs were stably expressed in NFAT-luciferase reporter Jurkat cells with mouse CD8 alpha and beta chains. Expression was verified by GFP and TCRβ (H57-597; BioLegend) staining. Various tumor cell lines expressing HER2 or not were plated overnight before Jurkat cells were added for 18 hours. After incubation, cells were lysed and measured using a Veritas microplate luminometer (Turner Biosystems). All samples run in quadruplicate.

Statistical analysis and data visualization

Data are presented as mean ± SEM. Tumor volumes, flow cytometry, ELISA, and ELISPOT data from experiments with three or more treatment groups were analyzed by one-way ANOVA with Bonferroni multiple comparisons test. Comparisons were made to untreated or control group unless otherwise indicated. A two-tailed, unpaired Student *t* test was used for experiments with only two groups. Group sizes for animal tumor growth experiments were determined on the basis of preliminary datasets. All subjects in spontaneous tumor experiments were randomized into a treatment or control group. Kaplan–Meier methods were used to generate time to event plots, and groups were compared using the log-rank test. Graphs were generated and statistical analysis was performed using Prism (GraphPad) and R. Script for R code for single-cell RNA-seq (scRNA-seq) can be found at https://github.com/cramanuj/Her2VAX. *P* values of 0.05 or less were considered statistically significant. Not all significant differences are shown in every graph. *, $P < 0.05$; **, $P < 0.01$; ***, $P < 0.001$.

Results

HER2Δ16 expression in breast cancer and its role in transformation and resistance to targeted therapies

Although HER2Δ16 has been reported to be expressed in many breast cancer cell lines, we wanted to determine its expression in patient samples to assess its potential as a molecular driver of breast cancer. There is currently no antibody that can distinguish these two isoforms at the protein level. As such, we utilized isoform-specific primers to measure expression of HER2 and HER2Δ16 in 154 different breast cancer specimens and 14 normal tissue specimens by qRT-PCR. Surprisingly, we found that HER2Δ16 expression was not only elevated in $HER2^+$ tissue, but was also elevated in tumor tissue expressing estrogen receptor (ER) and/or progesterone receptor (PR; **Fig. 1A**). HER2Δ16 accounted for approximately 10% of total HER2 transcripts in all of these samples (**Fig. 1B**).

To assess the oncogenic impact of HER2Δ16 on canonical cellular signaling pathways, we stably transduced cells with doxycycline-inducible expression of GFP, HER2WT, HER2Δ16, as well as a truncated form of HER2Δ16 that expresses only the extracellular portion (HER2Δ16-EC) and a HER2Δ16 with a point mutation in the ATP-binding site that renders the kinase domain inactive (HER2Δ16-KI; Supplementary Fig. S1A). Using these cells, we tested the impact of these genes on 43 different canonical signaling pathways using a luciferase tagged transcription factor reporter system. GFP and HER2WT did not induce any of the pathways, but HER2Δ16 stimulated high transcriptional activity of five different signaling pathways (MAPK/ERK, MAPK/JNK, PKC/Ca++, EGR, and Hedgehog; **Fig. 1C**). MAPK, PKC, and EGR pathways are all canonically expressed downstream of HER-family dimers (25–27), supporting the hypothesis that the HER2Δ16 isoform is functioning as a constitutively active homodimer (28). The Hedgehog pathway has not previously been associated with HER2 signaling but has been shown to play a role in other subtypes of breast cancer, particularly in the epithelial–mesenchymal transition (EMT) and may represent a novel downstream effect of HER2Δ16 expression (29, 30). Importantly, truncation or mutation of HER2Δ16 completely abrogates signaling through these pathways (**Fig. 1C**).

We next investigated whether HER2Δ16 expression transformed the nonmalignant murine mammary cell lines MM3MG and NMUMG. After identical stable transduction and selection, we found that HER2Δ16 had consistently lower expression than HER2WT on the surface of these cells despite identical promoters (Supplementary Fig. S1B). HER2Δ16 expression conferred significantly enhanced anchorage-independent growth *in vitro*, even with this reduced expression (**Fig. 1D**; Supplementary Fig. S1C). Furthermore, expression of HER2Δ16, but not HER2WT, allowed for robust tumor formation when these cells were implanted in mice (**Fig. 1E**). These results demonstrate that HER2Δ16 can effectively transform murine mammary cells, despite lower levels of expression.

Consistent with other studies, we observed that antibody-dependent cytotoxicity (ADCC) by the conventional HER2-targeting therapy trastuzumab and cell-mediated lysis by trastuzumab-DM1 (T-DM1) were reduced in HER2Δ16-expressing cells, compared with HER2-WT (**Fig. 1F** and **G**). Furthermore, HER2Δ16-expressing tumor cells were completely resistant to TDM1 treatment *in vivo* (**Fig. 1H**). This suggests that clinical HER2Δ16 expression could enhance tumor growth signaling and result in decreased efficacy of HER2-targeting therapies. Thus, our data support that HER2Δ16 expression may represent an important mechanism of resistance to these standard-of-care (SOC) therapies and critical target for immunotherapy in refractory $HER2^+$ breast cancers (28, 31).

Endogenous model of HER2Δ16-driven breast cancer as a model of $HER2^+$, immunosuppressive tumors with low tumor mutational burden

We have previously described a mouse model that utilizes a doxycycline-inducible promoter to drive expression of HER2Δ16 and

Published OnlineFirst July 30, 2020; DOI: 10.1158/1078-0432.CCR-20-0389

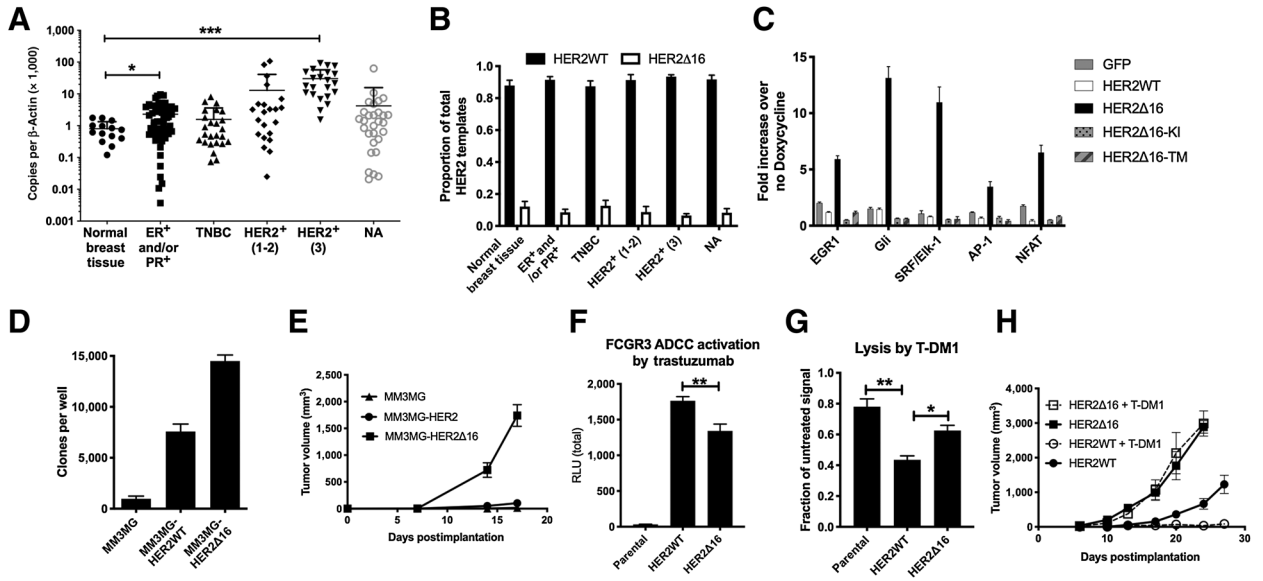

Figure 1.

The HER216 isoform is expressed in patient samples, transforms cell lines, and can be targeted immunologically using a viral vaccine platform. **A,** Human breast cancer cDNA arrays were analyzed for expression of the HER2Δ16 isoform by qPCR. β-ctin was used as an endogenous control. Normal ($n = 14$), ER/PR ($n = 56$), TNBC ($n = 25$), HER2$^+$ 1–2 ($n = 22$), HER2$^+$ 3 ($n = 22$), no information available (NA; $n = 29$). **B,** Arrays from **A** were also analyzed for expression of full-length HER2 transcripts and the proportion of total HER2 transcripts accounted for the full-length (WT) or HER2Δ16 isoform is shown. **C,** 293T cells were stably transduced with doxycycline-inducible GFP, HER2-WT, HER2Δ16, HER2Δ16-KI (kinase inactivated), or HER2Δ16-ECD (extracellular domain). Cells were transfected with luciferase reporter constructs for EGR1, Gl1, SRF/Elk-1, AP-1, or NFAT pathways and treated with dox or not for 48 hours to induce HER2 expression. Luciferase in cell lysates was measured and is shown as fold increase over no dox controls. $n = 4$. **D,** MM3MG cells were stably transduced with HER2-WT or HER2Δ16 and grown in soft agar and colonies were counted after 7 days. $n = 20$. **E,** MM3MG cells were implanted subcutaneously in SCID-beige mice. Caliper measurements converted to tumor volumes are shown. $n = 5$. **F,** NMUMG cells were plated overnight and incubated with 1 μg/mL of trastuzumab antibody for 1 hour prior to adding FCGR3-NFAT-luciferase expressing Jurkat reporter cells for 18 hours. Jurkat cells were lysed and luciferase expression is shown. $n = 4$. **G,** NMUMG cells were plated with 6.5 μg/mL T-DM1 or left untreated for 3 days. Cell growth was measured using an MTT assay. Data shown as fraction of untreated signal. $n = 3$. **H,** MM3MG cells expressing either HER2WT or HER2Δ16 were implanted subcutaneously in SCID-beige mice. When tumors formed, half of each cohort received 15 mg/kg of T-DM1 intravenously weekly and the rest remained untreated. Caliper measurements converted to tumor volumes are shown. $n = 5$. Error bars, SEM. *, $P < 0.05$; **, $P < 0.01$; ***, $P < 0.001$. **C** and **D** representative of six independent experiments; **E–H** representative of two independent experiments.

EGFP. When bred to MMTV-tTA (21) or MMTV-rtTA mice (20), these inducible models express HER2Δ16 in basal and luminal mammary epithelial cells, inducing multifocal, HER2Δ16$^+$ tumors in approximately 30% of MMTV-tTA mice and approximately 85% of MMTV-rtTA (**Fig. 2A**). Withdrawal of doxycycline results in loss of HER2Δ16 expression and complete tumor regression (Supplementary Fig. S1D), demonstrating the critical nature of HER2Δ16 in tumorigenesis. To evaluate the genetic identity of these tumors, RNA and DNA of four distinct tumors from different mammary glands in four different mice (total of 16 tumors) was sequenced and analyzed. These analyses revealed an elevated HER2-enriched subtype signature score (32) compared with other mouse models (Supplementary Table S1A), consistent with that found in human HER2$^+$ breast cancer and Erbb2/*neu* mouse tumors, generated by expression of the rat form of HER2 that develop spontaneous mutations in the juxtamembrane region (**Fig. 2B**). In addition, there was a significantly enhanced immunosuppression score (22) and myeloid-derived suppressor cell (33) score, highlighting the immunosuppressive TME present in these mice compared with other mouse models.

As these tumors are all driven by expression of the same oncogene, we next evaluated the similarity between the spontaneous tumors formed within the same mouse compared with tumors formed in different mice. This analysis revealed that distinct tumors from the same mouse were more genetically similar to other tumors from that same mouse than to tumors that formed in a different mouse (**Fig. 2C**). As neoepitope burden has been shown to correlate with immunogenicity and responsiveness to immune therapies, we employed next-generation DNA-seq and RNA-seq to determine the tumor mutational burden (TMB) and neoepitope load in these spontaneous tumors (22). We found that the TMB averaged only 0.57 mutations/MB (**Fig. 2D**). This corresponded to a very small number of predicted neoepitopes, with only one neoepitope with strong predicted MHCI binding potential and six additional with moderate binding potential present between all 16 sequenced tumors (Supplementary Table S1B). Collectively, these studies indicate that HER2Δ16 is a critical oncogenic pathway and spontaneous tumors driven by HER2Δ16 are reflective of clinically advanced immunosuppressive HER2$^+$ breast cancer.

Generation of antitumor immunity with kinase-inactivated HER2Δ16 viral vaccine

To direct immunity against HER2Δ16 without the risk of inducing an oncogenic signaling pathway, we generated an adenoviral vaccine encoding an inactivating mutation (K753A) in the kinase domain of HER2Δ16 (34). We found that a single vaccination of HER2 transgenic (HER2-Tg) mice with this vector elicited significant HER2-specific T-cell (**Fig. 3A**) and antibody responses (**Fig. 3B**). Moreover, these antibody responses were highly polyclonal, consisting of multiple isotypes, capable of stimulating ADCC and complement-dependent cell cytotoxicity (**Fig. 3C–E**). This HER2-specific immunogenicity was

Published OnlineFirst July 30, 2020; DOI: 10.1158/1078-0432.CCR-20-0389

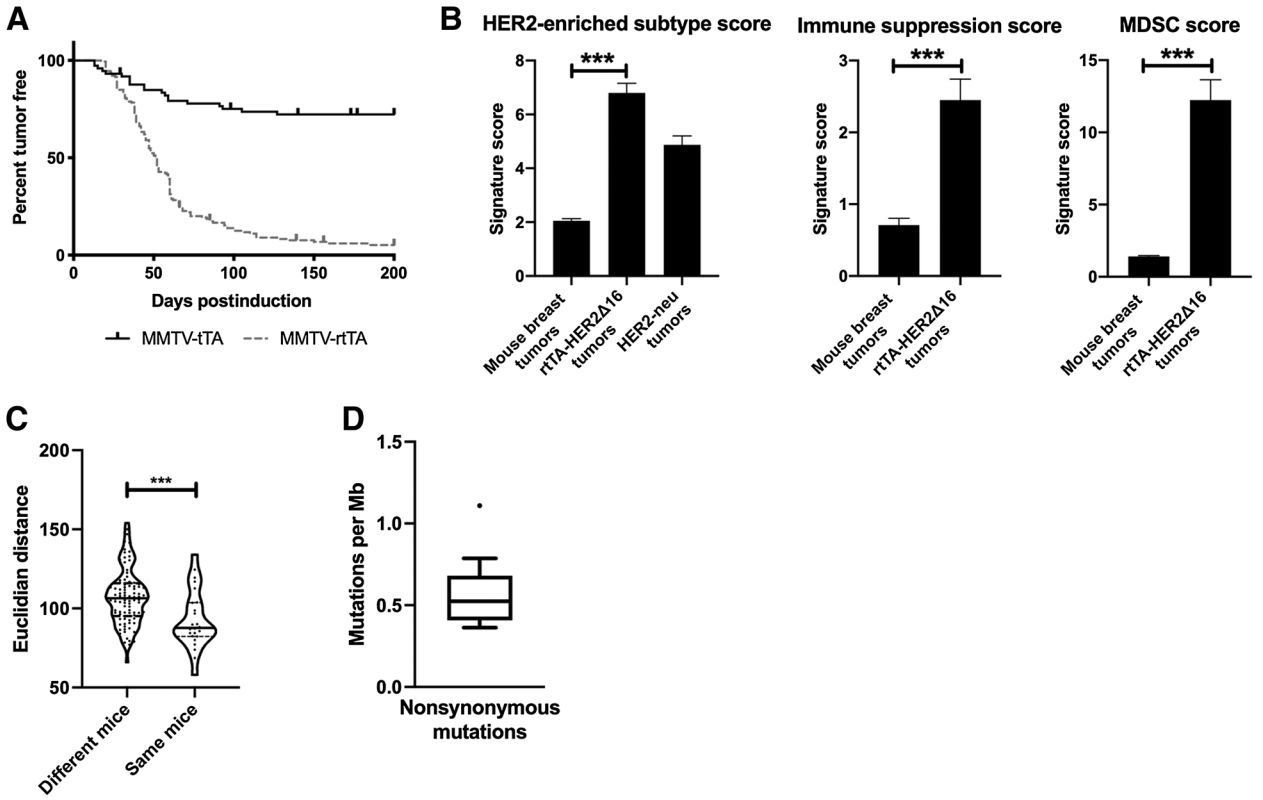

Figure 2.

Spontaneous HER2Δ16-driven breast tumors have HER2-enriched, immunosuppressive molecular signatures, and low mutational burden. **A,** Mice with a doxycycline-inducible promoter driving expression of HER2Δ16 and EGFP in the mammary epithelium were bred to MMTV-tTA or MMTV-rtTA mice and monitored for tumor formation. Percentage of tumor-free mice is shown. $n = 73$ for tTA and $n = 166$ for rtTA. **B,** Signature scores for RNA sequencing of four distinct tumors from different mammary glands in four different mice (total of 16 tumors) from rtTA-HER2Δ16 mice. **C,** Euclidian distance for each gene from tumors sequenced in **B** was compared for tumors from different mice and tumors taken from the same mice. **D,** DNA sequencing of samples from **B** was used to calculate nonsynonymous mutational burden for all 16 tumors compared with matched tail DNA samples and is shown as mutations per Mb of DNA. Box represents the 25th–75th percentile and whiskers represent ± 1.5 times the interquartile range. For all other plots, error bars indicate SEM. ***, $P < 0.001$.

not limited to these HER2-Tg mice, but was also seen in all other strains of mice tested (Supplementary Fig. S2).

To determine whether these HER2Δ16-specific immune responses could inhibit tumor growth, we orthotopically implanted MM3MG cells expressing HER2Δ16 (**Fig. 1E**) and vaccinated 3 days after implantation. Ad-HER2Δ16-KI vaccinated mice had a significant antitumor response compared with an irrelevant Ad-GFP control vaccine (**Fig. 3F**). Notably, the suppression of tumor growth correlated with an induction of both HER2-specific T-cell and antibody responses (**Fig. 3G** and **H**). These studies validated that our vaccine could elicit significant HER2-specific immunity against HER2Δ16 expressing tumors and slow their growth. However, this implantable tumor model grew too rapidly for long-term studies.

Efficacy of targeting HER2Δ16 versus neoepitope peptides or nononcogenic cancer-specific antigen

To perform long-term immunologic studies, we returned to our inducible HER2Δ16 model. The presence of EGFP and development of specific neoepitopes also allowed us to evaluate whether immunologic targeting of HER2Δ16 using our Ad-HER2Δ16 vaccine would be sufficient to elicit effective antitumor immunity relative to a neoepitope peptide vaccine (Supplementary Table S1B) or an identical viral vaccine targeting a coexpressed nondriver tumor antigen (GFP). To further identify which domain of HER2Δ16 provided the best tumor suppression, we engineered additional HER2Δ16-specific vaccines targeting the intracellular (ICD) and extracellular domains (ECDs).

We first evaluated the ability of these vaccine regimens to suppress tumor development when given early, before the establishment of palpable tumors. In this setting, we found that both the Ad-HER2Δ16-KI and the Ad-HER2Δ16-ECD vaccines were highly effective at suppressing tumor formation (**Fig. 4A**). However, neither Ad-HER2Δ16-ICD nor Ad-GFP were effective at delaying the appearance of tumors, with tumor formation identical to untreated and irrelevant vaccine (Ad-LacZ) treated mice (**Fig. 4A**). As Ad-GFP elicited potent anti-GFP responses (Supplementary Fig. S3A–S3C), but none of the GFP-expressing tumors were delayed in growth, we conclude that targeting a nononcogenic tumor antigen is not an effective therapeutic strategy. Similarly, vaccines targeting only the ICD of HER2 did not have a protective effect (**Fig. 4A**). As an additional comparison of the impact of targeting a coexpressed nondriver tumor antigen like GFP in an implantable tumor model, we engineered our MM3MG-HER2Δ16–expressing cells to also express GFP and vaccinated mice after implantation of these cells. Again, the vaccine targeting HER2Δ16 significantly delayed tumor growth compared with one targeting GFP in this implantable tumor model (Supplementary Fig. S4A).

Published OnlineFirst July 30, 2020; DOI: 10.1158/1078-0432.CCR-20-0389

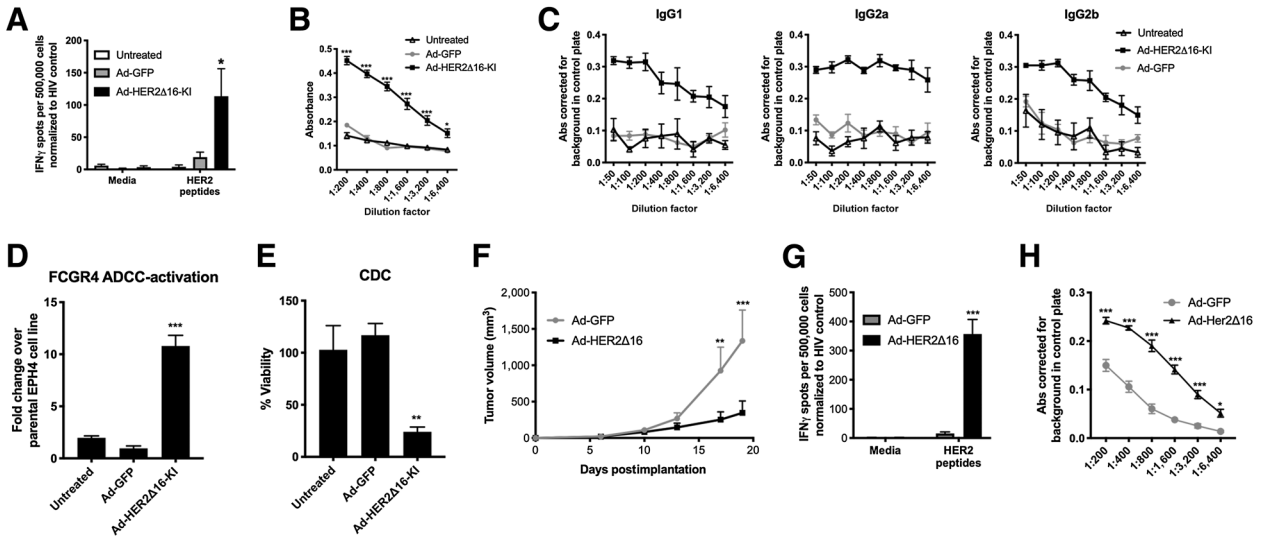

Figure 3.

Ad-HER2Δ16 vaccine induces potent T-cell and polyfunctional antibody responses that inhibit tumor growth. HER2-Tg mice were vaccinated with Ad-HER2Δ16-KI in the footpad and 2 weeks later spleens and serum were harvested. **A,** Splenocytes were stimulated with indicated peptides and IFNγ-producing cells were analyzed by ELISPOT. $n = 5$–7. **B,** Serum was analyzed by cell based ELISA for anti-HER2 specific total IgG antibodies. **C,** Serum from **B** was analyzed by same cell based ELISA for indicated IgG isotype. **D,** EPH4 cells expressing HER2 or not were plated overnight and incubated with serum from **B** for 1 hour prior to adding FCGR4-NFAT-luciferase expressing Jurkat reporter cells for 18 hours. Jurkat cells were lysed and luciferase expression is shown as fold change over parental cell line. **E,** Luciferase expressing MM3MG-HER2Δ16 or parental cells were incubated with serum from **B** for 1 hour. After incubation, rabbit serum was added as a source of complement for 4 hours. Cells were lysed and luciferase was measured. Data shown as percent of control cells incubated with heat-inactivated serum. **F,** MM3MG cells were implanted into the mammary fat pad of HER2-Tg mice and vaccines were given 3 days postimplantation. Caliper measurements converted to tumor volumes are shown. $n = 5$. **G,** Splenocytes from mice in **F** were stimulated with indicated peptides at the terminal endpoint and IFNγ-producing cells were analyzed by ELISPOT. **H,** Serum from mice in **F** was analyzed by cell-based ELISA for anti-HER2–specific total IgG antibodies. Error bars, SEM. *, $P < 0.05$; **, $P < 0.01$; ***, $P < 0.001$. **A–E** represent two independent experiments; **F–H** represent three independent experiments.

Vaccines targeting neoantigens have been shown to be effective in other tumor models (35). Neoepitopes identified when sequencing tumors were targeted with a peptide vaccine and compared with peptides from GFP and HER2 (Supplementary Table S1B). Vaccination against both neoepitope and GFP peptides once again had no effect, while HER2 peptides were able to delay tumor formation (Supplementary Fig. S4B).

To evaluate the role of each arm of the adaptive immune system in the protection elicited by vaccination, we depleted CD8 T cells or B cells and tracked the formation of tumors following vaccination with Ad-HER2Δ16-KI. Delay of tumor formation by vaccination was completely lost when CD8 T cells were depleted, while B-cell depletion had no impact on the time or proportion of mice that developed tumors (**Fig. 4D**). Although CD8 depletion was complete and sustained, it should be noted that despite initial B-cell depletion, the populations of B cells rebounded to normal levels even with prolonged weekly treatment of depleting antibodies (Supplementary Fig. S4C–S4E). Collectively, these data highlight the critical role that CD8 T cells play in the protection elicited by our vaccine.

To better model the impact of immunotherapy in patients with advanced $HER2^+$ breast cancer, we evaluated the efficacy of vaccination in mice with an established tumor. Mice were placed on doxycycline and once tumors reached approximately 100 mm^3, were randomized into different treatment arms. We found that while Ad-HER2Δ16-KI significantly increased survival of mice and generated robust anti-HER2 T-cell immunity, in this setting, all treated mice still ultimately succumbed to tumors (**Fig. 4E** and **F**). Consistent with our early vaccine studies, we found that vaccination targeting HER2Δ16 significantly enhanced responses compared to targeting the tumor antigen GFP (**Fig. 4E**). To determine whether earlier oncogene induction would elicit enhanced immune tolerance and alter the efficacy of vaccination, we repeated this experiment in MMTV-tTA mice, where expression is induced immediately after weaning by discontinuing doxycycline treatment. However, despite this early expression, we again observed the same pattern of efficacy (Supplementary Fig. S4F and S4G).

In summary, we found that vaccination is able protect 75% of mice from tumor formation when given prior to overt tumor formation and significantly slows tumor growth after measurable tumors have formed. However, vaccination alone was never able to achieve a complete cure. Thus, although these studies reveal that immunologic targeting of HER2Δ16 is effective at combating tumor formation and progression, they also highlight that the induction of tumor-specific T-cell responses alone is not enough to eradicate advanced breast cancer.

Role of the PD-1–PD-L1 axis in mediating local HER2Δ16 breast cancer immunosuppression

One possible explanation for the inability of our HER2-targeting vaccine to eradicate tumors is the regulatory effect of PD-1-PD-L1 signaling in the TME. To test this and establish the role of PD-1-PD-L1 immunosuppression in our $HER2^+$ breast cancer models, we evaluated rtTA-HER2Δ16 tumors and found that both $HER2^+$ tumor cells (**Fig. 5A**) and myeloid populations from the tumors including monocytes and neutrophils (**Fig. 5B**) expressed high levels of PD-L1. To determine the potential of this pathway in mediating antitumor immunosuppression, we first investigated the role of tumor cell PD-L1 expression. Using an implantable tumor model, we again observed elevated tumor-specific expression

Published OnlineFirst July 30, 2020; DOI: 10.1158/1078-0432.CCR-20-0389

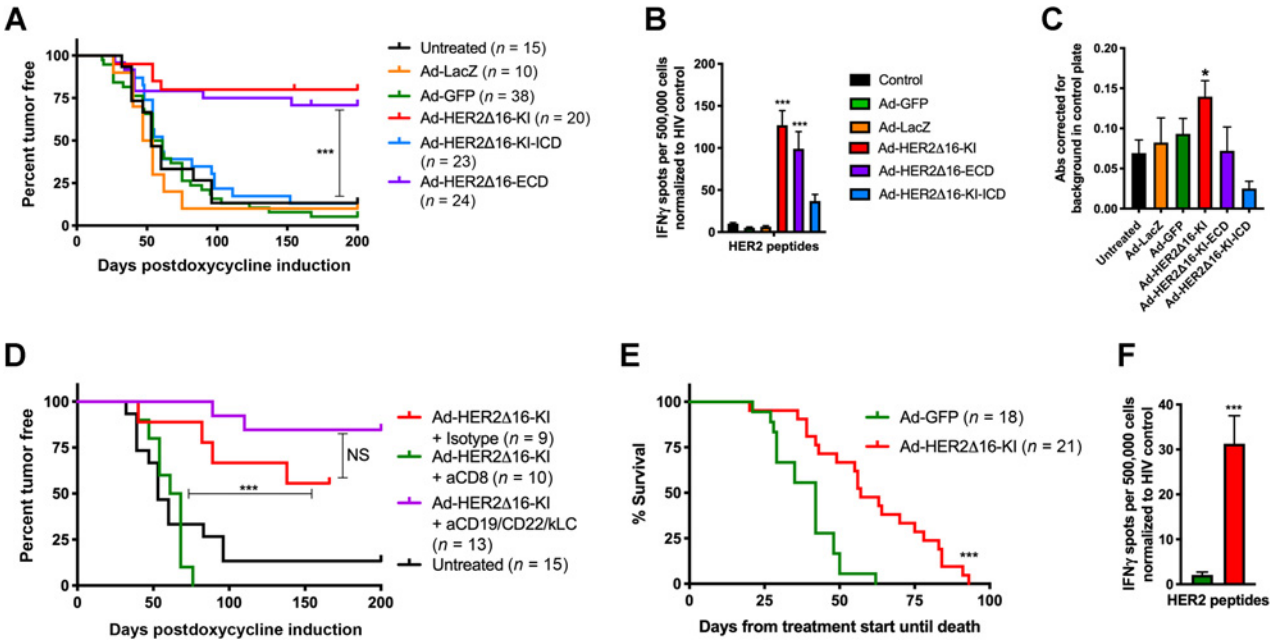

Figure 4.

Vaccination targeting the extracellular domains of HER2Δ16 can prevent the occurrence of tumors and therapeutically treat existing tumors in a CD8 T-cell–dependent manner. **A,** rtTA-HER2Δ16 mice were given dox food for 1 week prior to vaccination. Mice were monitored for tumor formation weekly and the percentage of tumor-free mice is shown. **B,** At terminal endpoint, splenocytes from **A** were stimulated with indicated peptides and IFNγ-producing cells were analyzed by ELISPOT. **C,** At terminal endpoint, serum from **A** was analyzed by cell-based ELISA for anti-HER2–specific total IgG antibodies. **D,** rtTA-HER2Δ16 mice were given dox food for 1 week prior to depleting antibody treatment. One week after initial depletion, mice were vaccinated with Ad-HER2Δ16-KI as before. Mice were monitored for tumor formation and treated with depleting antibodies weekly and the percentage of tumor-free mice is shown. **E,** rtTA-HER2Δ16 mice were given dox food and monitored for tumor formation weekly. Once a palpable (>200 mm^3) tumor was detected, mice were randomized into a treatment group and vaccinated. Mice were sacrificed when tumors reached a terminal volume. **F,** At terminal endpoint, splenocytes from **E** were stimulated with indicated peptides and IFNγ-producing cells were analyzed by ELISPOT. Error bars, SEM. *, $P < 0.05$; **, $P < 0.01$; ***, $P < 0.001$. All experiments are representative of a rolling enrollment and longitudinal analysis.

of PD-L1 (**Fig. 5C**). After ablation of tumor PD-L1 using CRISPR lentiviruses (**Fig. 5C**), we observed that PD-L1-KO cells grew much more poorly compared with controls (**Fig. 5D**). This growth difference, however, did not result in an enhancement of systemic HER2-specfic T-cell or B-cell responses (**Fig. 5E** and **F**), suggesting that this axis altered local T-cell responses. Consistent with these results, treatment of MM3MG-HER2Δ16 tumors with αPD-1 antibodies significantly slowed tumor growth and continued treatment resulted in tumor regression in most mice (**Fig. 5G**), but did not significantly enhance systemic HER2-specific T-cell responses or B-cell responses (**Fig. 5H** and **I**). Collectively, these results suggest that the PD-1-PD-L1 axis plays a critical immunosuppressive role in HER2Δ16-driven cancers and that its blockade is sufficient to cause significant tumor regression in an implantable tumor model of $HER2^+$ cancer where significant anti-HER2 immune responses are present.

Synergistic impact of HER2Δ16 immunologic targeting enabled by PD-1 immune checkpoint blockade

Although αPD-1 demonstrated efficacy in an orthotopic model, we wanted to assess the impact of αPD-1 alone and in combination with HER2Δ16 vaccination in a more immunosuppressive context, as occurs in advanced $HER2^+$ breast cancer. Using HER2Δ16 transgenic mice with established $HER2^+$ tumors, we administered αPD-1 alone or in combination with Ad-HER2Δ16-KI. In contrast to our orthotopic $HER2Δ16^+$ breast cancer model, we found that endogenous $HER2^+$ breast cancers did not respond to αPD-1 as a single agent (**Fig. 6A**). Likewise, treatment with αPD-1 was insufficient to increase systemic anti-HER2 T-cell responses (**Fig. 6B**). However, the combination of αPD-1 and Ad-HER2Δ16-KI resulted in a significant enhancement in survival, with approximately 30% of mice exhibiting complete tumor regression and long-term (>150 days) tumor-free survival (**Fig. 6A**). Interestingly, the addition of αPD-1 treatment did not further enhance the systemic HER2-specific T-cell response above what was seen with vaccine alone (**Fig. 6B**). This suggested that the difference in antitumor efficacy of the combination therapy was again occurring within the TME.

To determine the effect of vaccination and ICB on the activity and clonal expansion of T cells in the TME, we utilized scRNA-seq to profile TILs from treated mice. Given the high rate of complete tumor regression and in an effort to minimize differences in tumor size, samples were collected within 3 weeks of enrolling in a given treatment arm. Tumors were digested and enriched for T cells prior to scRNA-seq for total gene expression and TCR genes. Overlaying the TCR libraries confirms our cluster identification of T cells (**Fig. 6C**; Supplementary Fig. S5). Furthermore, by identifying clones that have expanded (>10 with a shared TCR sequence), we see that nearly all expanded clones are contained within a single cluster (activated CD8 T cells). We focused our analysis on the gene expression of cells with a corresponding TCR sequence and utilized previously published gene signatures (Supplementary Table S1C) to examine the immunologic properties of cells from each treatment groups. Predictably, TILs from mice that had received the viral Ad-

Published OnlineFirst July 30, 2020; DOI: 10.1158/1078-0432.CCR-20-0389

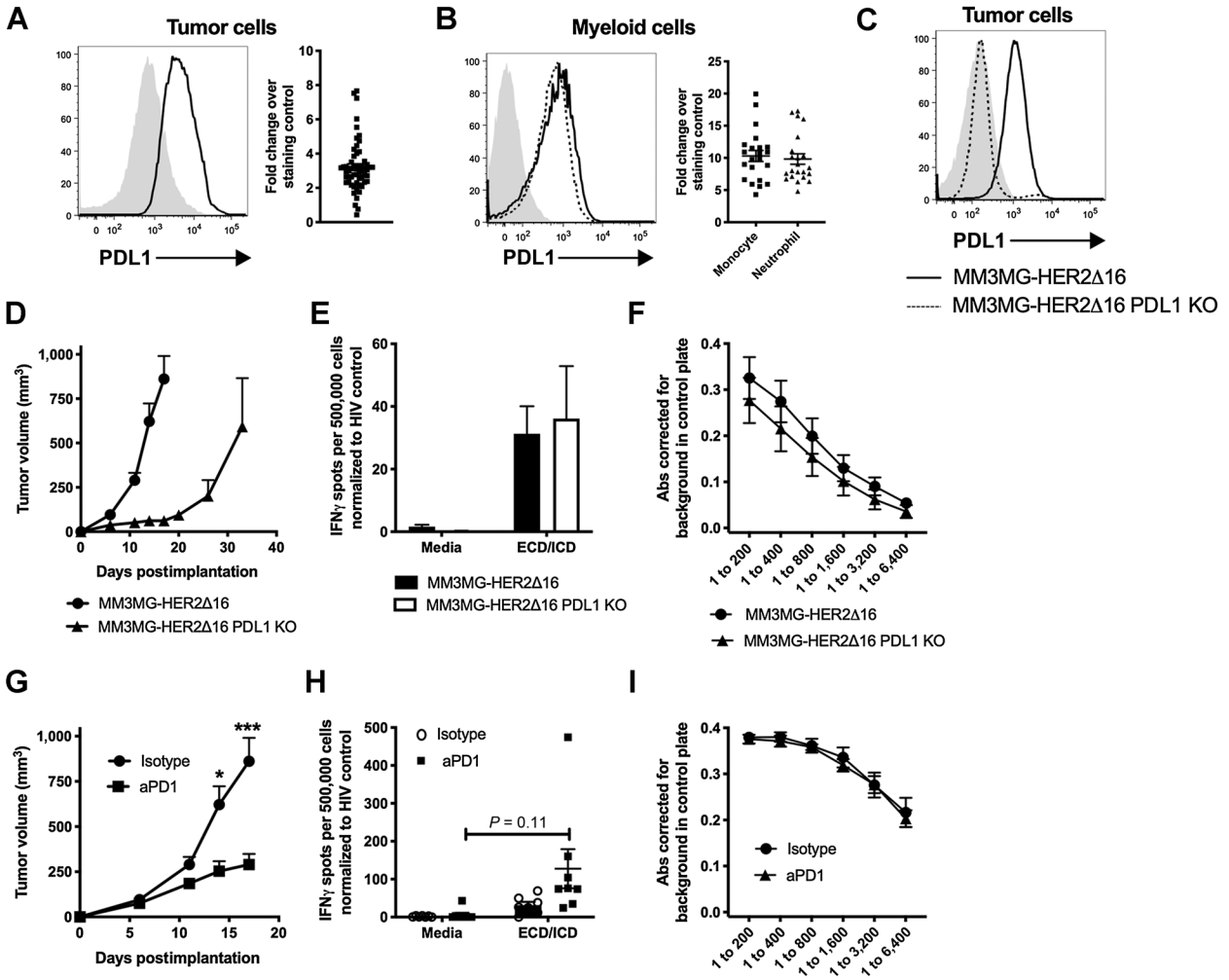

Figure 5.

The PD-1 pathway is critical for HER2Δ16-driven tumor growth and treatment with PD-1–blocking antibodies is highly effective at abrogating tumor growth. rtTA-HER2Δ16 mice were given dox food and monitored for tumor formation weekly. Mice were sacrificed when tumors reached a terminal volume and tumors were digested for analysis by flow cytometry. Digested tumors were plated overnight and adherent tumor cell were stained for PD-L1 expression (**A**) or stained fresh for immune cell markers and PD-L1 (**B**). Cells in **A** are pregated on live, $CD45^-$, $HER2^+$ ($n = 57$ tumors). Cells in **B** were pregated on live, $CD45^+$, $CD11b^+$, $Ly6C^+$ (monocyte), or $Ly6G^+$ (neutrophil; $n = 22$ tumors). **C,** PD-L1 expression on MM3MG-HER2Δ16 cells before and after ablation with CRISPR. **D,** MM3MG-HER2Δ16 and MM3MG-HER2Δ16-PD-L1 KO cells were implanted into the mammary fat pad of HER2-Tg mice. Caliper measurements converted to tumor volumes are shown. $n = 7$. **E,** At terminal endpoint, splenocytes from **D** were stimulated with indicated peptides and IFNγ-producing cells were analyzed by ELISPOT. **F,** At terminal endpoint, serum from **D** was analyzed by cell-based ELISA for anti-HER2–specific total IgG antibodies. **G,** MM3MG-HER2Δ16 cells were implanted into the mammary fat pad of HER2-Tg mice and mice were treated twice weekly with intraperitoneal injection of 200 μg/mouse anti–PD-1. Caliper measurements converted to tumor volumes are shown ($n = 7$–8). **H,** At terminal endpoint, splenocytes from **G** were stimulated with indicated peptides and IFNγ-producing cells were analyzed by ELISPOT. **I,** At terminal endpoint, serum from **G** was analyzed by cell-based ELISA for anti-HER2–specific total IgG antibodies. Error bars, SEM. *, $P < 0.05$; **, $P < 0.01$; ***, $P < 0.001$. **A** and **B** represent data compiled from two experiments. **D–F** are representative of two independent experiments. **G–I** are representative of two independent experiments.

HER2Δ16 vaccine, regardless of the addition of αPD-1, showed significant expression of proinflammatory and type I IFN pathways (**Fig. 6D**). Strikingly, in mice that only received the vaccine, this robust immune activation was also coupled with a significant and profound increase in immune dysfunction pathways including anergy and coinhibitory molecule expression (**Fig. 6D**). Given this dichotomy, we generated an activation and exhaustion signature based on genes that were differentially expressed with known activation (TNFα, IFNγ) and exhaustion (Havcr2, Lag3 Tigit) markers (**Fig. 6E**; Supplementary Table S1D). These scores once again confirm greatly enhanced activation in both vaccine groups, with a correspondingly high exhaustion score in vaccine alone that is diminished when αPD-1 is added to the vaccine. Finally, a gene signature of IFNγ-associated genes has been published as a predictor of responsiveness to αPD-1 therapy in patients (36). Consistent with this report, our data confirm a high IFNγ gene signature score in vaccinated mice.

Interestingly, we saw evidence of expanded clones in unvaccinated mice, which led us to question the specificity of the TILs in these samples. With the paired TCR alpha and beta chain sequence

Published OnlineFirst July 30, 2020; DOI: 10.1158/1078-0432.CCR-20-0389

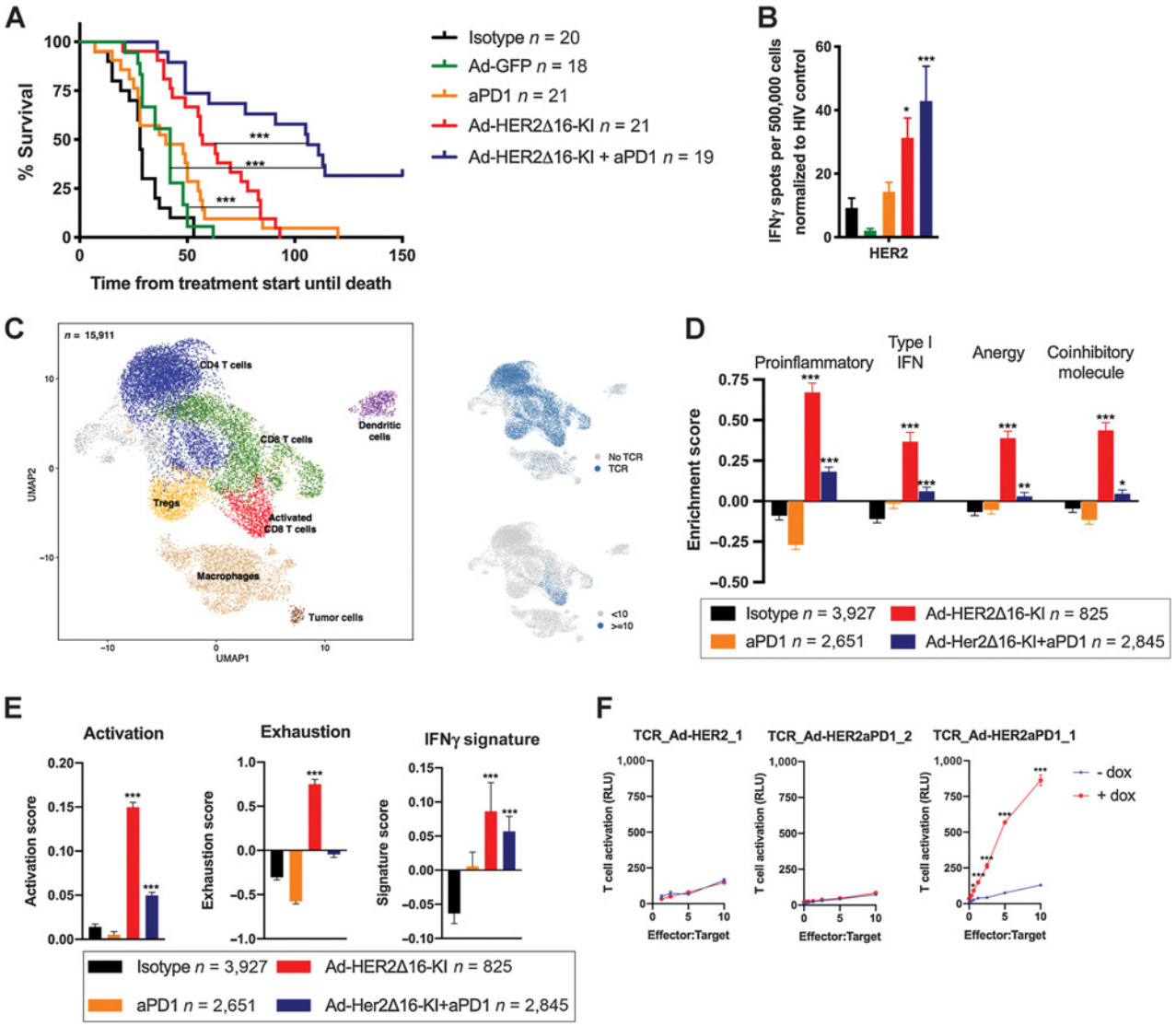

Figure 6.

Combination of aPD-1 and Ad-HER2Δ16-KI results in significantly enhanced survival, enrichment of proinflammatory and activation signatures while decreasing exhaustion. **A,** rtTA-HER2Δ16 mice were given dox food and monitored for tumor formation weekly. Once a palpable (>200 mm^3) tumor was detected, mice were randomized into a treatment group and vaccinated or given antibody intraperitoneally. Mice were sacrificed when tumors reached a terminal volume. **B,** At terminal endpoint, splenocytes from **A** were stimulated with indicated peptides and IFNγ-producing cells were analyzed by ELISPOT. **C,** Tumors were harvested within 3 weeks of starting therapy, digested, and live, single T cells sorted for analysis using 10x Genomics. Uniform manifold approximation and projection (UMAP) of all cells with clusters of inferred cell types are shown. UMAP colored by TCR detection (top right) or expanded clones >10 (bottom right). **D,** Enrichment scores for all cells with corresponding TCR (signatures obtained from previously published studies). **E,** Activation and exhaustion scores (based on expression of top 50 genes most correlated with GzmB or HAVCR2 expression) and the signature score 6-gene IFNγ score (previously published). **F,** TCRs from expanded clones were expressed in NFAT-luc reporter Jurkat cells incubated with cells expressing HER2Δ16 or not to test for TCR specificity. Target cells are HER2Δ16-expressing cells from a tumor taken from rtTA-HER2Δ16 mice that were treated with doxycycline (red) or not (blue). RLU, relative luminometer units. Error bars, SEM. *, $P < 0.05$; **, $P < 0.01$; ***, $P < 0.001$.

data from our scRNA-seq (Supplementary Table S1E), we cloned the TCRs from the top expanded clone from mice that had received a vaccine or not into NFAT-luciferase reporter Jurkat cells. We then screened these TCRs using a tumor cell line created from an rtTA-HER2Δ16 spontaneous tumor that had retained the dox-dependent expression of HER2Δ16. Strikingly, we were able to demonstrate that the expanded clone from an Ad-HER2Δ16 vaccinated mouse was highly reactive to HER2 (**Fig. 6F**). We confirmed this reactivity in several other HER2Δ16-expressing cell lines (Supplementary Fig. S6). Collectively, these results demonstrate the ability of HER2Δ16 vaccination to not only induce systemic adaptive immune responses, but expand HER2-specific CD8 T cells that infiltrate into tumors. Thus, our model of established, immunosuppressive tumors (similar to those seen clinically) demonstrates that the addition of αPD-1 can effectively enable vaccinated induced HER2-specific T cells in the TME.

Published OnlineFirst July 30, 2020; DOI: 10.1158/1078-0432.CCR-20-0389

Discussion

HER2$^+$ breast cancer comprises approximately 15% to 20% of all breast cancer cases and is typified by amplification of HER2 expression (37). Here, we have demonstrated that the oncogenic HER2Δ16 comprises approximately 10% of HER2 transcripts but confers exceptionally enhanced oncogenic signaling to tumor cells and resistance to standard-of-care mAb therapies (**Fig. 1**). In patients with metastatic HER2$^+$ breast cancer, acquired resistance to these is inevitable, and nearly all patients will die of disease progression even though tumors continue to express HER2 (38). Recent clinical trials utilizing αPD-1 in patients with breast cancer have revealed only modest response rates, with the highest responses being in TNBC. On the basis of these findings, we hypothesized that specific immunologic targeting of the HER2Δ16 isoform may offer an effective therapeutic strategy for metastatic and/or treatment-resistant HER2$^+$ breast cancer, which could be rationally combined with PD-1/PD-L1 mAbs.

To explore this hypothesis, we generated a novel viral vaccine vector to elicit HER2-specific adaptive immune responses, without oncogenic signaling (critical for vaccine safety). Using an implantable model, we have shown that both our novel vaccine and αPD-1 ICB were highly effective, which was in contrast to the endogenous HER2Δ16$^+$ breast cancer model, where neither single agent achieved complete tumor regression. Although we utilized HER2-Tg animals and orthotopic implantation into the mammary fat pad, implantation of tumor cells alone appeared able to break tolerance and stimulate an anti-HER2 response, possibly caused by cell death and release of damage-associated molecular patterns (DAMPs) during implantation, foreign residual FBS proteins from tissue culture, or from the rapid growth of these tumors. Conversely, we did not observe striking anti-HER2Δ16 immune responses in transgenic animals bearing endogenous tumors, indicating a level of tolerance that is more consistent with the muted response rates seen in patients (39). This aspect of the study supports the use of transgenic models for immunotherapy research and suggests that studies relying upon orthotopic implantation of tumor cells may exaggerate immune agent responsiveness.

Our study also directly tested the efficacy of a vaccine targeting an oncogene versus a nononcogenic tumor antigen (GFP). Importantly, we found that vaccination against HER2Δ16 or the ECD of this gene, was far more effective at protecting from tumor formation and eliciting significantly prolonged survival of tumor bearing mice (**Fig. 4**). This is in contrast to vaccination against a gene that was still specific to the tumor but did not play any role in transformation (GFP), which had no protective or therapeutic effect. These studies highlight the potential difference of directing immune responses against antigens that are credentialed tumor drivers, versus tumor-specific antigens or private neoepitopes that do not play a significant role in oncogenesis to increase the success and translatability of immunotherapies, particularly in cancers with a low TMB and few neoepitopes to target.

We also leveraged our inducible transgenic model to explore the impact of tumor progression and timing on the effectiveness of our vaccine strategy. Although the size and progression of tumors are generally thought to alter responsiveness to antitumor immunity (40), few studies have directly tested whether outcomes differ in an endogenous tumor setting after identical immunologic interventions. Our studies illustrate that vaccinations during early tumor development prior to any overt tumor formation are highly effective, but are drastically suppressed once a larger immunosuppressive TME has formed. This is significant for the clinical use of these therapies where early-phase clinical trials almost exclusively focus on late-stage metastatic patients, who have progressed on all conventional therapies. These data provide evidence that failure of immune therapies in this advanced patient population does not predict how effective that therapy may be in an earlier stage of the disease. Our studies also reveal that the PD-1–PD-L1 axis plays a critical role in this immunosuppressive phenotype in HER2Δ16-driven breast cancer. Notably, the use of αPD-1 in established disease was not effective at suppressing tumor growth (∼0% >150 day survival rate), despite the presence of TILs and expression of PD-1 and PD-L1 in various cell types within the TME, consistent with what has been reported clinically (**Figs. 4A** and **6A**). This observation is somewhat at odds with the premise that tumors with high expression of PD-L1 should be more responsive to αPD-1/PD-L1 therapies. In bladder cancer, PD-L1 expression by nontumor cells in the TME is more associated with clinical response to PD-L1 inhibition, which highlights the need to better define biomarkers for these ICB therapies within specific cancer types (41, 42).

Cancer immunotherapy is in an era where monotherapies are often promising but subtherapeutic for most patients and the challenge remains to devise rational combinations that will maximize the benefit and curative potential. Much work has been done to test various tumor antigen targeting vaccine strategies and checkpoint inhibitors, with many showing evidence of CD8 T-cell activation (43–45). Consistent with these studies we show that our HER2Δ16 vaccine in combination with αPD-1 had a synergistic curative effect (**Fig. 6A**). Mechanistically, scRNA-seq analysis revealed that TILs from mice receiving vaccine alone exhibited a broad program of immune dysfunction including upregulation of anergy, coinhibitory molecule expression, and exhaustion pathways. It is important to note that these pathways were upregulated early, as the scRNA-seq samples for vaccine alone were harvested only 15 days postvaccination. Coinhibitory molecule expression is one of the markers of an exhausted CD8 T-cell population that distinguishes it from a function memory or effector CD8 T cells (46). Although exhaustion has been the main focus of ICB therapy in cancer, tolerance of T cells toward specific antigens, or T-cell anergy, may develop due to TCR stimulation without sufficient costimulatory signals or in the presence of inhibitory stimulation. T-cell anergy may develop in our model and in cancer more generally because coinhibitory signals prevail over costimulatory signals in the complex milieu of the TME (47). The induction of an exhaustion signature is consistent with a previous report investigating CD8 TILs in patients with carcinoma after PD-1 blockade (48). Overall, our data highlight and provide single cell evidence for why vaccines for cancer may not be potent enough to combat advanced disease as single agents.

The ability to sequence the paired TCRα/β chains from single cells provides an unprecedented opportunity to understand the specificity of cells that are generated by vaccination and infiltrating into the TME. We leveraged this technology by cloning of the expanded TCRα/β chains and subsequent *in vitro* assays to demonstrate that our vaccine not only expanded T cells, but the expanded clones are specific for HER2 epitopes (**Fig. 6F**). Other groups have utilized similar techniques to evaluate expansion of vaccine and tumor-specific T cells in PBMCs (49, 50), but here we show the expansion of vaccine-induced antigen-specific T cells taken directly from the tumor. Although this observation is exactly what we would predict based on the established vaccine paradigm and observations of PBMC responses reported by others, it is an important proof-of-concept experiment that elegantly demonstrates this foundational premise in a endogenous model of advanced cancer. It further provides a basis for investigation of the specificity of expanded T cells in tumors or infectious diseases, which may provide critical information about the accuracy of

Published OnlineFirst July 30, 2020; DOI: 10.1158/1078-0432.CCR-20-0389

immunodominance predictions and the level of bystander "nonspecific" infiltration that occurs.

The success of PD-1/PD-L1 immune checkpoint blockade has renewed interest in clinical immunotherapy, spurred efforts to identify what defines a responsive patient population, and prompted the testing of combinatorial strategies to improve patient response rates. Most of these efforts have centered on pairing αPD-1/PD-L1 mAbs with standard-of-care therapies (radiation, chemotherapy, etc.) and different immune checkpoint blockade antibodies (i.e., CTLA4, TIM3, LAG3, etc.). In our study, we demonstrate that a vaccine targeting a nonmutated oncogene isoform (HER2Δ16) is effective in mobilizing antitumor T-cell responses that can then be effectively enabled by an αPD-1 mAb to elicit complete tumor regression and long-term tumor-free survival. As such, we believe that this approach offers a rational paradigm for precision immunity through the use of oncogene targeted vaccines in combination with selective ICB mAbs. Although our study has only tested the impact of this combination in $HER2^+$ breast cancer, future preclinical studies may extend this framework to other cancers where HER2 is highly expressed (such as gastric cancer) or more critically, to other oncogene targets (such as EGFR, c-myc, etc.). Clinically, these promising studies have led to the initiation of a phase II clinical trial testing a similar novel HER2 vaccine (targeting the HER2 ECD in an alphaviral particle) in combination with pembrolizumab (NCT03632941) to determine whether this approach can elicit effective antitumor immunity while minimizing off-target immune responses in patients with advanced $HER2^+$ breast cancer.

Disclosure of Potential Conflicts of Interest

L.A. Chodosh reports grants from Breast Cancer Research Foundation and NIH during the conduct of the study, as well as personal fees from Imerys Talc America (expert witness in cancer litigation), Sterigenics, Inc (consultant in cancer litigation), U.S. Department of Justice (expert witness in cancer litigation), Arnold & Porter, LLP (consultant in cancer litigation), Takeda, Inc (expert witness in cancer litigation), and Janssen Pharmaceuticals (consultant in cancer litigation) outside the submitted work. G. Broadwater reports grants from NIH during the conduct of the study. T. Hyslop reports grants from NCI during the conduct of the study, as well as personal fees from AbbVie outside the submitted work. C.M. Perou reports personal fees from Bioclassifier LLC (equity stock holder and consultant of BioClassifier LLC) outside the submitted work, as well as ownership of a patent for U.S. Patent No. 12,995,459 issued, licensed, and with royalties paid from Bioclassifier LLC. B.G. Vincent reports personal fees from GeneCentric Therapeutics outside the submitted work. J. Force reports Consulting from Exact Sciences, Pfizer, Myriad, and NanoString Biotechnologies. M.A. Morse reports grants from Merck, BMS, AstraZeneca, personal fees from Taiho, Exelixis, Bayer, Novartis, and Roche/Genentech, and grants and personal fees from Eisai and Ipsen outside the submitted work. H.K Lyerly reports AlphaVax (equity) outside the submitted work, as well as membership of the Board of Directors of OncoSec. Z.C. Hartman and H.K. Lyerly report a patent WO2017120576A1 on cancer vaccines and methods of delivery, owned by Duke University and optioned to license to a Duke spin-out (Replicate Bioscience, Inc.). No potential conflicts of interest were disclosed by the other authors.

Authors' Contributions

E.J. Crosby: conceptualization, data curation, formal analysis, funding acquisition, visualization, writing-original draft. **C.R. Acharya:** formal analysis, visualization, writing-review and editing. **A.-F. Haddad:** methodology, writing-review and editing. **C.A. Rabiola:** investigation, writing-review and editing. G. Lei: resources, investigation, writing-review and editing. **J.-P. Wei:** investigation, writing-review and editing. **X.-Y. Yang:** investigation, writing-review and editing. **T. Wang:** investigation, writing-review and editing. **C.-X. Liu:** investigation, writing-review and editing. **K.-U. Wagner:** resources, writing-review and editing. **W.J. Muller:** resources, funding acquisition, writing-review and editing. **L.A. Chodosh:** resources, writing-review and editing. **G. Broadwater:** conceptualization, formal analysis. **T. Hyslop:** conceptualization, formal analysis. **J.H. Shepherd:** resources, data curation, formal analysis, writing-review and editing. **D.P. Hollern:** resources, data curation, formal analysis. **X. He:** resources, data curation, formal analysis. **C.M. Perou:** resources, data curation, writing-review and editing. **S. Chai:** resources, data curation, formal analysis. **B.K. Ashby:** resources, data curation, formal analysis. **B.G. Vincent:** resources, funding acquisition, writing-review and editing. **J.C. Snyder:** resources, validation, writing-review and editing. **J. Force:** writing-review and editing. **M.A. Morse:** writing-review and editing. **H.K. Lyerly:** supervision, funding acquisition, project administration, writing-review and editing. **Z.C. Hartman:** conceptualization, supervision, funding acquisition, writing-original draft, project administration, writing-review and editing.

Acknowledgments

This work was supported by the Susan G. Komen Foundation (CCR14299200 to Z. C. Hartman; PDF17481657 to E.J. Crosby; CCR17483467 to B.G. Vincent), Merck Sharp-Dohme Investigator Initiated Grant (LKR160831 to Z.C. Hartman), Department of Defense (BC113107 and BC132150 to H.K. Lyerly), NCI (5K12CA100639-09 to H.K. Lyerly and Z.C. Hartman, 1R01CA238217-01A1 to Z.C. Hartman, 5K12-CA100639-10 to H.K. Lyerly and J.C. Snyder, K22CA212058 to J.C. Snyder), Cancer Research Society (No. 21068 to W.J. Muller), and Canadian Institutes of Health Research (FND-148373 to W.J. Muller).

The costs of publication of this article were defrayed in part by the payment of page charges. This article must therefore be hereby marked *advertisement* in accordance with 18 U.S.C. Section 1734 solely to indicate this fact.

Received January 30, 2020; revised April 17, 2020; accepted June 25, 2020; published first July 30, 2020.

References

1. Havel JJ, Chowell D, Chan TA. The evolving landscape of biomarkers for checkpoint inhibitor immunotherapy. Nat Rev Cancer 2019;19:133–50.
2. Hamm CA, Moran D, Rao K, Trusk PB, Pry K, Sausen M, et al. Genomic and immunological tumor profiling identifies targetable pathways and extensive CD8+/PDL1+ immune infiltration in inflammatory breast cancer tumors. Mol Cancer Ther 2016;15:1746–56.
3. Michaut M, Chin S-F, Majewski I, Severson TM, Bismeijer T, de Koning L, et al. Integration of genomic, transcriptomic and proteomic data identifies two biologically distinct subtypes of invasive lobular breast cancer. Sci Rep 2016; 6:18517.
4. McGranahan N, Furness AJS, Rosenthal R, Ramskov S, Lyngaa R, Saini SK, et al. Clonal neoantigens elicit T cell immunoreactivity and sensitivity to immune checkpoint blockade. Science 2016;351:1463–9.
5. Wein L, Luen SJ, Savas P, Salgado R, Loi S. Checkpoint blockade in the treatment of breast cancer: current status and future directions. Br J Cancer 2018;119:4–11.
6. Dawood S, Rugo HS. Targeting the host immune system: PD-1 and PD-L1 antibodies and breast cancer. Curr Opin Support Palliat Care 2016;10: 336–42.
7. Nanda R, Chow LQM, Dees EC, Berger R, Gupta S, Geva R, et al. Pembrolizumab in patients with advanced triple-negative breast cancer: phase Ib KEYNOTE-012 study. J Clin Oncol 2016;34:2460–7.
8. Narang P, Chen M, Sharma AA, Anderson KS, Wilson MA. The neoepitope landscape of breast cancer: implications for immunotherapy. BMC Cancer 2019; 19:200.
9. Moasser MM, Krop IE. The evolving landscape of HER2 targeting in breast cancer. JAMA Oncol 2015;1:1154–61.
10. Arteaga CL, Engelman JA. ERBB receptors: from oncogene discovery to basic science to mechanism-based cancer therapeutics. Cancer Cell 2014; 25:282–303.
11. Kwong KY, Hung MC. A novel splice variant of HER2 with increased transformation activity. Mol Carcinog 1998;23:62–8.

12. Siegel PM, Ryan ED, Cardiff RD, Muller WJ. Elevated expression of activated forms of Neu/ErbB-2 and ErbB-3 are involved in the induction of mammary tumors in transgenic mice: implications for human breast cancer. EMBO J 1999; 18:2149–64.
13. Castiglioni F, Tagliabue E, Campiglio M, Pupa SM, Balsari A, Ménard S. Role of exon-16-deleted HER2 in breast carcinomas. Endocr Relat Cancer 2006;13: 221–32.
14. Turpin J, Ling C, Crosby EJ, Hartman ZC, Simond AM, Chodosh LA, et al. The ErbB2DeltaEx16 splice variant is a major oncogenic driver in breast cancer that promotes a pro-metastatic tumor microenvironment. Oncogene 2016;35:6053–64.
15. Tsao L-C, Crosby EJ, Trotter TN, Agarwal P, Hwang B-J, Acharya C, et al. CD47 blockade augmentation of trastuzumab antitumor efficacy dependent on antibody-dependent cellular phagocytosis. JCI Insight 2019;4:e131882.
16. Morse MA, Clay TM, Colling K, Hobeika A, Grabstein K, Cheever MA, et al. HER2 dendritic cell vaccines. Clin Breast Cancer 2003;3:S164–72.
17. Schneble EJ, Berry JS, Trappey FA, Clifton GT, Ponniah S, Mittendorf E, et al. The HER2 peptide nelipepimut-S (E75) vaccine (NeuVax) in breast cancer patients at risk for recurrence: correlation of immunologic data with clinical response. Immunotherapy 2014;6:519–31.
18. Crosby EJ, Gwin W, Blackwell K, Marcom PK, Chang S, Maecker HT, et al. Vaccine-induced memory CD8(+) T cells provide clinical benefit in HER2 expressing breast cancer: a mouse to human translational study. Clin Cancer Res 2019;25:2725–36.
19. Piechocki MP, Ho YS, Pilon S, Wei WZ. Human ErbB-2 (Her-2) transgenic mice: a model system for testing Her-2 based vaccines. J Immunol 2003;171: 5787–94.
20. Gunther EJ, Belka GK, Wertheim GBW, Wang J, Hartman JL, Boxer RB, et al. A novel doxycycline-inducible system for the transgenic analysis of mammary gland biology. FASEB J 2002;16:283–92.
21. Sakamoto K, Schmidt JW, Wagner KU. Generation of a novel MMTV-tTA transgenic mouse strain for the targeted expression of genes in the embryonic and postnatal mammary gland. PLoS One 2012;7:e43778.
22. Kardos J, Chai S, Mose LE, Selitsky SR, Krishnan B, Saito R, et al. Claudin-low bladder tumors are immune infiltrated and actively immune suppressed. Jci Insight 2016;1.
23. Smith CC, Chai S, Washington AR, Lee SJ, Landoni E, Field K, et al. Machine-learning prediction of tumor antigen immunogenicity in the selection of therapeutic epitopes. Cancer Immunol Res 2019;7:1591–604.
24. Stuart T, Butler A, Hoffman P, Hafemeister C, Papalexi E, Mauck WM, et al. Comprehensive integration of single-cell data. Cell 2019;177:1888–902.
25. Hudis CA. Drug therapy: Trastuzumab - Mechanism of action and use in clinical practice. N Engl J Med 2007;357:39–51.
26. Dillon RL, Brown ST, Ling C, Shioda T, Muller WJ. An EGR2/CITED1 transcription factor complex and the 14-3-3 sigma tumor suppressor are involved in regulating ErbB2 expression in a transgenic-Mouse model of human breast cancer. Mol Cell Biol 2007;27:8648–57.
27. Lyu H, Han A, Polsdofer E, Liu S, Liu BL. Understanding the biology of HER3 receptor as a therapeutic target in human cancer. Acta Pharmaceutica Sinica B 2018;8:503–10.
28. Mitra D, Brumlik MJ, Okamgba SU, Zhu Y, Duplessis TT, Parvani JG, et al. An oncogenic isoform of HER2 associated with locally disseminated breast cancer and trastuzumab resistance. Mol Cancer Ther 2009;8:2152–62.
29. Riobo-Del Galdo NA, Montero AL, Wertheimer EV. Role of Hedgehog signaling in breast cancer: pathogenesis and therapeutics. Cells 2019;8:375.
30. Kasper M, Jaks V, Fiaschi M, Toftgard R. Hedgehog signalling in breast cancer. Carcinogenesis 2009;30:903–11.
31. Tilio M, Gambini V, Wang J, Garulli C, Kalogris C, Andreani C, et al. Irreversible inhibition of Delta 16HER2 is necessary to suppress Delta 16HER2-positive breast carcinomas resistant to Lapatinib. Cancer Lett 2016;381:76–84.
32. Pfefferle AD, Herschkowitz JI, Usary J, Harrell J, Spike BT, Adams JR, et al. Transcriptomic classification of genetically engineered mouse models of breast cancer identifies human subtype counterparts. Genome Biol 2013;14:R125.
33. Youn J-I, Collazo M, Shalova IN, Biswas SK, Gabrilovich DI. Characterization of the nature of granulocytic myeloid-derived suppressor cells in tumor-bearing mice. J Leukoc Biol 2012;91:167–81.
34. Hartman ZC, Wei J, Osada T, Glass O, Lei G, Yang X-Y, et al. An adenoviral vaccine encoding full-length inactivated human Her2 exhibits potent immunogenicty and enhanced therapeutic efficacy without oncogenicity. Clin Cancer Res 2010;16:1466–77.
35. Ott PA, Dotti G, Yee C, Goff SL. An update on adoptive T-cell therapy and neoantigen vaccines. Am Soc Clin Oncol Educ Book 2019;39:e70–8.
36. Ayers M, Lunceford J, Nebozhyn M, Murphy E, Loboda A, Kaufman DR, et al. IFN-γ–related mRNA profile predicts clinical response to PD-1 blockade. J Clin Invest 2017;27:2930–40.
37. Nuciforo P, Radosevic-Robin N, Ng T, Scaltriti M. Quantification of HER family receptors in breast cancer. Breast Cancer Res 2015;17:53.
38. Vicario R, Peg V, Morancho B, Zacarias-Fluck M, Zhang J, Martínez-Barriocanal Á, et al. Patterns of HER2 gene amplification and response to anti-HER2 therapies. PLoS One 2015;10:e0129876.
39. Drake CG, Jaffee E, Pardoll DM. Mechanisms of immune evasion by tumors. Adv.Immunol 2006;90:51–81.
40. Ogiya R, Niikura N, Kumaki N, Bianchini G, Kitano S, Iwamoto T, et al. Comparison of tumor-infiltrating lymphocytes between primary and metastatic tumors in breast cancer patients. Cancer Sci 2016;107:1730–5.
41. Bellmunt J, Mullane SA, Werner L, Fay AP, Callea M, Leow JJ, et al. Association of PD-L1 expression on tumor-infiltrating mononuclear cells and overall survival in patients with urothelial carcinoma. Ann Oncol 2015;26:812–7.
42. Cristescu R, Mogg R, Ayers M, Albright A, Murphy E, Yearley J, et al. Pan-tumor genomic biomarkers for PD-1 checkpoint blockade-based immunotherapy. Science 2018;362:eaar3593.
43. Curran MA, Glisson BS. New hope for therapeutic cancer vaccines in the era of immune checkpoint modulation. Annu Rev Med 2019;70:409–24.
44. van Montfoort N, Borst L, Korrer MJ, Sluijter M, Marijt KA, Santegoets SJ, et al. NKG2A blockade potentiates CD8 T cell immunity induced by cancer vaccines. Cell 2018;175:1744–55.
45. Ali OA, Lewin SA, Dranoff G, Mooney DJ. Vaccines combined with immune checkpoint antibodies promote cytotoxic T-cell activity and tumor eradication. Cancer Immunol Res 2016;4:95–100.
46. Wherry EJ, Kurachi M. Molecular and cellular insights into T cell exhaustion. Nat Rev Immunol 2015;15:486–99.
47. Crespo J, Sun H, Welling TH, Tian Z, Zou W. T cell anergy, exhaustion, senescence, and stemness in the tumor microenvironment. Curr Opin Immunol 2013;25:214–21.
48. Yost KE, Satpathy AT, Wells DK, Qi Y, Wang C, Kageyama R, et al. Clonal replacement of tumor-specific T cells following PD-1 blockade. Nat Med 2019; 25:1251–9.
49. Hu Z, Anandappa AJ, Sun J, Kim J, Leet DE, Bozym DJ, et al. A cloning and expression system to probe T-cell receptor specificity and assess functional avidity to neoantigens. Blood 2018;132:1911–21.
50. Takeda K, Kitaura K, Suzuki R, Owada Y, Muto S, Okabe N, et al. Quantitative T-cell repertoire analysis of peripheral blood mononuclear cells from lung cancer patients following long-term cancer peptide vaccination. Cancer Immunol Immunother 2018;67:949–64.

Published OnlineFirst July 30, 2020; DOI: 10.1158/1078-0432.CCR-20-0389

Clinical Cancer Research

Stimulation of Oncogene-Specific Tumor-Infiltrating T Cells through Combined Vaccine and αPD-1 Enable Sustained Antitumor Responses against Established HER2 Breast Cancer

Erika J. Crosby, Chaitanya R. Acharya, Anthony-Fayez Haddad, et al.

Clin Cancer Res Published OnlineFirst July 30, 2020.